A Far-Field Evaluation Method for Interfacial Defects Existed in Composite Insulators Based on Transient Thermal Wave

SIDA ZHANG[1], **CHENJUN GUO**[2], **LI CHENG**[1], **(Member, IEEE), AND HANQING WANG**[1]

[1]State Key Laboratory of Power Transmission Equipment & System Security and New Technology, Chongqing University, Chongqing 400044, China
[2]Yunnan Electric Power Research Institute, China Southern Power Grid, Kunming 530100, China

Corresponding author: Li Cheng (chengl16@cqu.edu.cn)

ABSTRACT The interfacial defect of composite insulators is common, which is majorly responsible for the fracture of insulators after the acid resistant core rod is used. Based on the active infrared detection method, the far-field evaluation method can effectively keep the operation safety of transmission lines by detecting subtle internal defects which are difficult to find by the traditional non-destructive detection methods. Above all, the propagation law of heat has been studied. The difference of the surface temperature between defective and reference area has been calculated when the thermal excitation meet the Dirac function. Second, the plate and short insulator samples with interfacial defects have been produced. The defects in plate samples could be easily distinguished by radiation quantity but not in insulators. In order to increase the resolution of experimental result, the derivate of the data has been further processed in the Logarithmic coordinate system. The difference between defective area and reference area has approximately enlarged 7 times and 1 mm defect in insulators, which is the smallest, could be distinguished. The detecting distance has been expanded from several millimeters to 50 centimeters which offers a possibility to the online application. Finally, according to the test results, a preliminary standard for thermal wave evaluation focused on the interfacial defects has been proposed.

INDEX TERMS Composite insulators, interfacial defect, non-destructive evaluation, thermal wave, transmission lines.

I. INTRODUCTION

Advantaged by light quality and outstanding resistance of contamination flashover, etc., the composite insulators have been extensively adopted in EHV and UHV transmission system [1]–[4]. As manufacture has been progressively matured and acid-resistance core rod has been widely adopted, traditional defects, e.g. brittle fracture, shall no longer make insecure the operation of composite insulators. Yet in recent years, a new type of fracture has occurred frequently. As the existing research indicates [5]–[7], this type of fracture is closely associated with interfacial defects of composite insulators, which is severely jeopardizing. Electric discharge and hydrolysis might be possibly triggered by interfacial defects and epoxy resin would be corroded by that. The corrosion of epoxy resin will further lead to exposure and fracture of glass fiber [8]–[9]. As a consequence, the mechanical strength of insulators shall be reduced.

Based on abundant researches, a lot of Non-destructive testing (NDT) and algorithm based methods [10]–[15] focus on the insulator defects has been proposed. However, the defects is difficult to detect online in certain distance with existing electromagnetic wave and ultrasonic detection methods. The current detection distance always ranges from several millimeters to centimeter which is not sufficient for the high voltage application. Using hand-held infrared thermal imager to detect the thermal radiation of energized composite insulators at long distance or near distance is a common detection method. However, it is a type of passive detection method only for energized insulators with low detection accuracy. It is hard to find defective insulators according to existing infrared detection standards [14].

Based on active infrared thermal-wave technology, the manuscript proposes a kind of far-field non-destructive detecting method for interfacial defects of composite
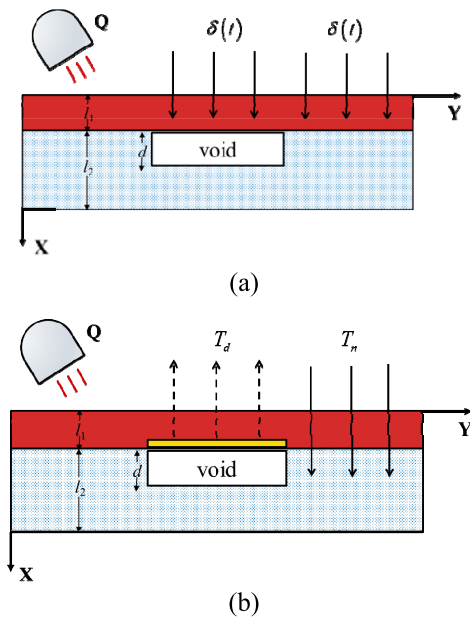
FIGURE 1. Spreading model of thermal wave in defective composite medium: (a) Before thermal wave reaches air gap defect; (b) After thermal wave reaches air gap defect.

insulators. First and foremost, modelling analysis is implemented on spreading principle of thermal wave in composite-medium with gap. Secondly, the test platform is established and theoretical result is further verified by test to plate samples. Eventually, the short insulator samples with interfacial defects are tested and the result are researched on the form of radiation curve. In order to increase the resolution of the result, the derivate of the data has been further processed in the Logarithmic coordinate system. As the test results indicate, identification precision of the method is 1mm and the detection distance is over 50 cm.

II. BACK GROUND

Given that defective thermal conductivity (normally referring to air), silicone rubber sheath materials and epoxy resin material differ from each other. Propagation law of heat flow in composite insulators shall be impacted by difference of thermal conductivity and discontinuous heat conduction in defect shall lead to discontinuous surface temperature field after imposing transient thermal excitation to the insulators. Accordingly, the distribution of surface temperature field shall be impacted by geometric dimension and heat conducting performance of different inner media and defects can be detected through adopting the infrared methods.

To delve into heat transmission process, a plate model has been established (Fig.1), as a first approximation, to equivalently describe physical model of heat transmission in defective insulator.

For transient thermal excitation, the heat flux can be approximated as a $\delta(t)$ function. Because the surface material has a small thermal conductivity, it takes a certain time before the thermal wave reaches the defect. The equivalent model is

shown in Fig.1.a. When the thermal wave reaches the surface of the defect, because the thermal conductivity of the air gap defect is significantly lower than that of the solid, the thermal wave cannot cross the air gap defect and a new heat source is formed on the surface of the defect in a short time (As shown in Fig.1.b). It can be considered that the thermal wave takes places in total reflection here.

In the analysis of spreading model of heat wave, the temperature T is solution of thermal conductivity differential equation in x direction at moment t [16].

$$\frac{\partial T(x, t)}{\partial t} = a \frac{\partial^2 T(x, t)}{\partial x^2} \left(a = \frac{k}{\rho c}\right) \quad (1)$$

a and k are thermal diffusivity and thermal conductivity respectively. ρ represents density; c indicates specific heat capacity. The difference of thermal properties between silicone rubber (SIR) and fiber reinforced polymer (FRP) is small and its effect on surface temperature is negligible, so the same thermal diffusivity and thermal conductivity can be used for calculation. For environment temperature T_0, the initial condition is satisfied as:

$$T(x, 0) = T_0 \quad (2)$$

In the meantime, surfaces in the model meet heat balance condition.

$$\delta(t) + k \frac{\partial T}{\partial x}|_{x=0} = h[T(0, t) - T_0]$$

$$k \frac{\partial T}{\partial x}|_{x=l_1+l_2} + h[T(l_1 + l_2, t) - T_0] = 0 \quad (3)$$

h is the convective heat transfer coefficient. Arising from short thermal wave detection, error of convective term to temperature distribution is less than 3% [17]; thus, it can be negligible. Temperature field distribution condition on silicone surface without defect (x = 0) could be attained by simultaneous 3 formulas.

$$T_{\mathrm{n}}(0, t) = T_0 + \frac{I_0}{(\pi \rho c k t)^{0.5}} \quad (4)$$

For the air gap defect in the sample, the equivalent conversion is carried out in the form of Fig.1.b. The calculated results of surface temperature are as follows.

$$T_d(0, t) = T_0 + \frac{I_0}{(\pi \rho c k t)^{0.5}} \left[1 + \exp\left(-\frac{l_1^2}{at}\right)\right] \quad (5)$$

Where, I_0 denotes unit area heat absorption when silicone rubber surface is exposed to radiation. Temperature difference with defect and without defect after neglecting edge condition can be solved following (6):

$$\Delta T = \frac{I_0}{(\pi \rho c_1 k_1 t)^{0.5}} \exp(-\frac{l_1^2}{at}) \quad (6)$$

As indicated, the temperature in defective position is higher than that in reference position; i.e. surface radiation distribution is uneven and inner defects can be judged through comparing difference of radiation volume among
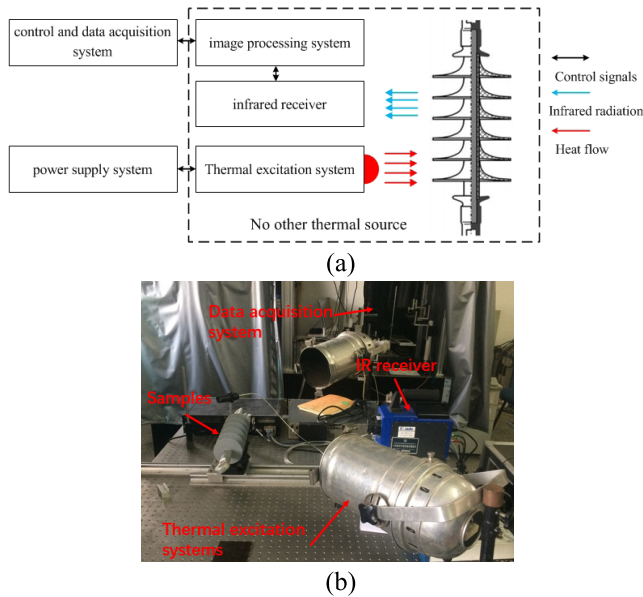
(a)

(b)

FIGURE 2. Working principle of the active thermography test:
(a) Schematic Diagram of Infrared Thermal Wave Detection;
(b) Infrared Thermal Wave Detection Test System (integral insulator was replaced by short samples in the experiment).

TABLE 1. Sample No. and specific information.

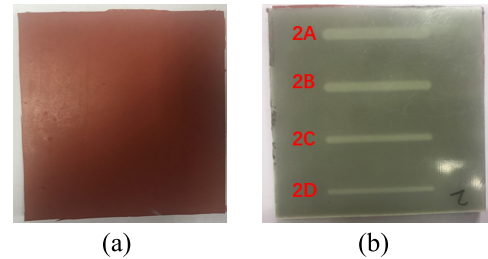| No.	Type	Thickness of defect	Amount
1	Plate	1mm	4
2	Plate	2mm	4
3	Insulator	0.5mm	1
4	Insulator	1mm	1
5	Insulator	2mm	1

(a)   (b)

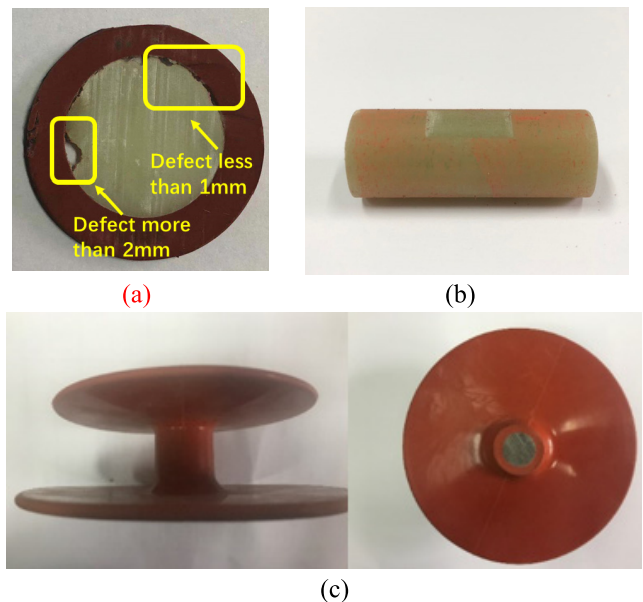**FIGURE 3.** Plate sample: (a) Silicone rubber side; (b) Epoxy board side.

(a)   (b)

(c)

FIGURE 4. Short insulator samples: (a) Typical air gap in insulators; (b) 1mm air gap defect; (c) Defective short sample.

surface areas. In the meantime, it is demonstrated that precision is associated with defect depth; the larger the defect depth, the smaller the temperature difference and the lower the judgment precision.

III. EQUIPMENT AND TEST METHOD

Test system (Fig.2) is comprised of thermal excitation system, infrared receiver, image processing system, power supply system and control/data acquisition system. Thermal excitation system is composed by 2 flashing lights, taking on the power of 5.9 kJ. The control/data acquisition system is connected with the infrared receiver and excitation system through communication interface. The image and radiant quantity are collected and processed by software. To detect interfacial defect of composite insulators, the certain heat has been imposed to samples within short time. The difference of radiation quantity can be distinguished by infrared receiver after heating and variation principle of thermal radiation quantity with time variation shall be analyzed.

Plate samples (Fig.3) and actual insulators (Fig.4) with different dimension defects have been studied in this paper. The relevant information and the No. of the samples are listed in Table 1.

Plate sample is composed by silicone rubber and epoxy resin plate. The silicone rubber is 3.5mm thick while epoxy resin is 3 mm thick. The type of coupling agent is KH-560. There are 4 different slots with different widths in the epoxy resin board, marked as A, B, C and D and being 4 mm, 3 mm, 2 mm and 1 mm in width, respectively. For instance, 2A represents the first slot on No.2 sample, i.e. the widest one (the width is 4mm). Due to certain transparency of the epoxy board, dimension information of defect can be clearly

seen through observing samples from epoxy board side. (As shown in Fig. 3.b).

The typical air gap in insulators is wide but shallow groove between the sheath and the core rod [13], [18]–[21] (as indicated in Fig.4.a). Currently it can be merely detected by dissection, which is a destructive method. In other words, the defects shall be exposed to the air when it was verified. The exposure of defect shall affect the heat diffusion process in samples evidently so that the distribution of surface temperature is changed. In order to avoid the case, artificial air defect isolated to the air has been produced in the interface.

To prevent defect from contacting with external air directly and keep the defect to the condition before dissection, a batch
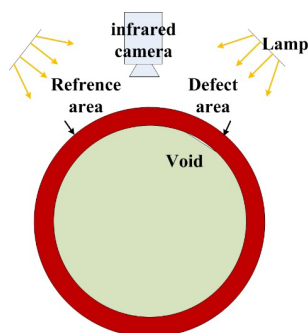
FIGURE 5. Measurements and arrangement method of short insulator sample.

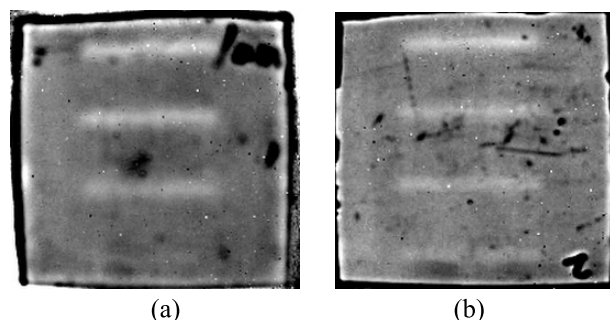(a)   (b)

FIGURE 6. Test result of radiation quantity of plate sample: (a) Radiation quantity of No.1 sample; (b) Radiation quantity of No.2 sample.

of insulators with air defects is manufactured specially; the diameter of the rod is 18mm while the thickness of sheath is 5.8mm thick. The primary manufacturing process is as follows:

1. Do not apply coupling agent on core rod surface, but inject silicone rubber on core rod to form silicone rubber sheath.

2. Extract core rod from sheath. To simulate sample, defects with different thickness are dug. (Fig. 4.b).

3. Apply coupling agent KH-560 on core rod surface (except for defects) and insert core rod to sheath again. Finally, solidify coupling agent with high temperature.

For air defect on cylinder interface, it can be denoted by maximum of defect depth. Fig.4.c presents the defective short sample manufactured and the inner defect cannot be observed directly.

In the actual detection process, because the specific location of the defect can not be determined, the defect is not directed at infrared camera in general, but with a certain angle. Considering the incident heat source, the point with the same incident energy can be found at the symmetrical position as reference (Fig.5).

IV. RESULTS AND DISCUSSION
A. TEST RESULT OF RADIATION QUANTITY

The distribution principle of surface radiation quantity of various samples can be obtained directly whereby test system. First and foremost, the plate samples is studied. The radiation

quantity of silicone rubber is presented in Fig. 6. As indicated, there is an evident strip hot spot on No. 2 samples, of which shape and position is consistent with defect and its radiation quantity is higher than reference area radiation quantity, which is consistent with calculation result of theoretical expression (6).

In the meantime, thickness of the defect exerts comparatively large impacts on detection precision. It is hard to identify the thinnest slot of No. 1 sample by radiation quantity directly, whereas the thinnest slot of No. 2 sample can be identified clearly. Besides, other than the theoretic calculation, dimension of defect vertical to heat wave incident direction (means the width of the slots) exerts certain influence on analysis precision of infrared heat wave. Edge effect and limit to inherent resolution of infrared detection are main causes of the influence. For composite insulators, general thickness of air gap is relatively shallow, whereas the width is relatively large (Fig. 4.a) and length of air gas found out in previous period basically outstrips 10mm (along rod axis length). Therefore, it can be analyzed by the heat diffusion process.

Sheath thickness of actual composite insulator is normally 3-6 mm [22], [23] and the sheath thickness of experimental sample is 5.8mm, which is much thicker than that of plate samples. To verify effectiveness of infrared thermal wave method on composite insulator, No.3, 4 and 5 insulators short samples has been detected. Its infrared detection result is shown in Fig.7. As indicated, for smaller defects (No.3 and No.4), during the whole thermal dissipation, it is hard to distinguish surface radiation difference brought by defects directly. Whereas for larger defect (No.5), it can be barely distinguished. Further, taking 3 points from reference and detective area for radiation analysis (see Fig.5 for reference). The sampling points are described in sample numbering-sampling area-sampling point numbering form. For instance, 5-D-1 is the first sampling point in defect area of No.5 sample. Fig.7 has provided variation principle of radiation quantity of defect and reference area of No. 3, No.4 and No.5 samples where full line is defect area and hidden line is reference area.

Through comparing the variation of radiation quantity between defective and reference area in Fig.7, as indicated, radiation quantity in defect area is higher than that in reference area. However, difference is very subtle and relative variation quantity of difference value is less than 5%, which is consistent with theoretical calculation result. According to (6), when defect depth (the thickness of sheath) increases, the surface temperature difference will decrease exponentially. Thus the requirements of actual measurement is difficult to satisfy. To meet the test conditions, it is necessary to further analyse the radiation quantity.

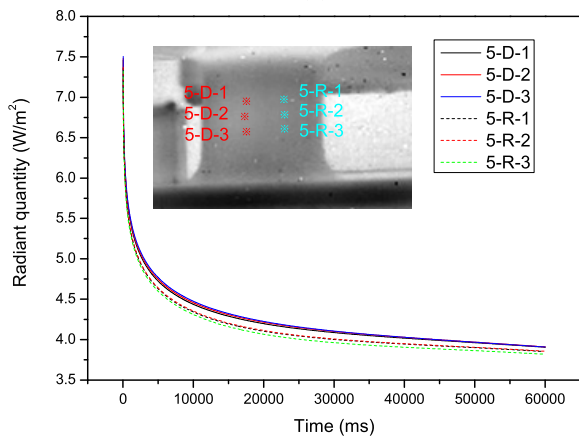### B. TEST RESULT OF THE RATE OF RADIATION QUANTITY

For thermal radiation, its radiation quantity R is proportional to the difference between the biquadrate of the surface temperature and environmental temperature which
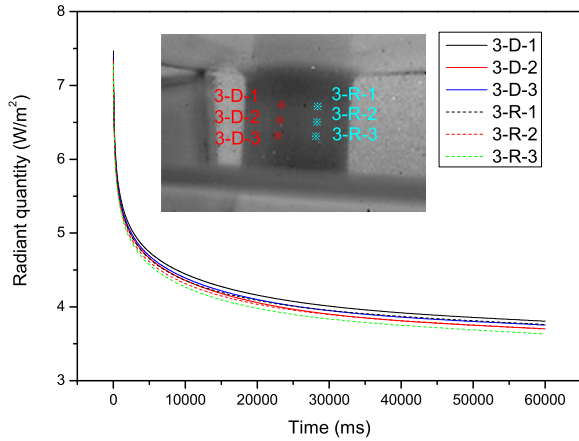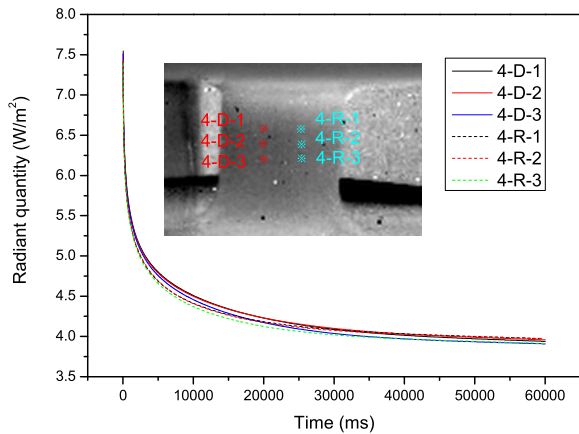
FIGURE 7. Radiation quantity of short insulators: (a) radiation quantity of No.3 sample; (b) radiation quantity of No.4 sample (c) radiation quantity of No.5 sample.

could be obtained by (7). ε is the infrared emittance and C_0 is the Black-body radiation coefficient which equals 5.67 W/(m^2·K^4):

$$R = \varepsilon C_0 (T_{SIR}^4 - T_0^4) \quad (7)$$

Therefore, radiation quantity is a curve that decreases quickly first and then decreases slowly which tends to be
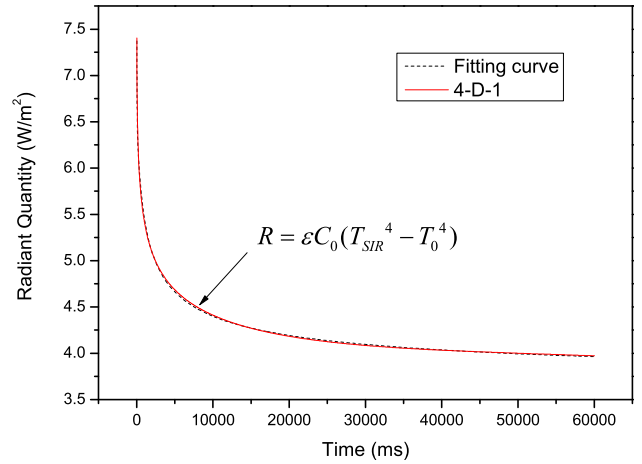

FIGURE 8. The fitting results of the radiant quantity of 4-D-1.

stable finally. The law of the radiation quantity over the time could be fitted by a quartic polynomial. Take 4-D-1 as an example, the fitting curve is consistent with the test result (Fig.8). But due to the difference between the propagation law of plate samples and insulator samples, there is some difference between the fitting coefficients and the actual parameters.

Because radiation quantity is characterized by quick variation and large difference in previous period and slow variation and small difference in latter period, which is applicable to analysis under logarithm coordinates. Besides, thermal dissipation process is further analyzed to improve detection precision and it is allowed to research influence of defect on variation rate of radiation quantity.

In summary, rule of variation rate of radiation quantity on time can be analyzed by taking natural logarithm to take the derivative of radiation quantity. Results are shown in Fig.9: As indicated, after derivation that radiation variation speed in non-defect area is lower than that in defect area during temperature fall period. Because thermal energy can keep balance quickly in inner object without air gap with much lower thermal conductivity, the temperature of non-defect sample can reach balance relatively quickly in the beginning of temperature decrease. Therefore, the variation is mostly relatively slow in latter period of temperature decrease process. It can be seen through comparing variation rate of radiation quantity (Fig.9) and radiation quantity (Fig.7) that result difference for samples with defect and without defect is more significant after derivation. It shall be highlighted that, due to the difference of location and relative heat source angle of different samples (virtually, during site measurement, relative heat source angles of different samples are hard to ensure to be identical), there is no comparability between results of different samples and influence of thermal wave result on sample position is very sensitive.

To compare precision of the two types of methods visually, taking minimum radiation quantity (as 5-R-3 in Fig.7.c) and absolute value of radiation variation rate (as 5-R-3 in Fig.9.c)
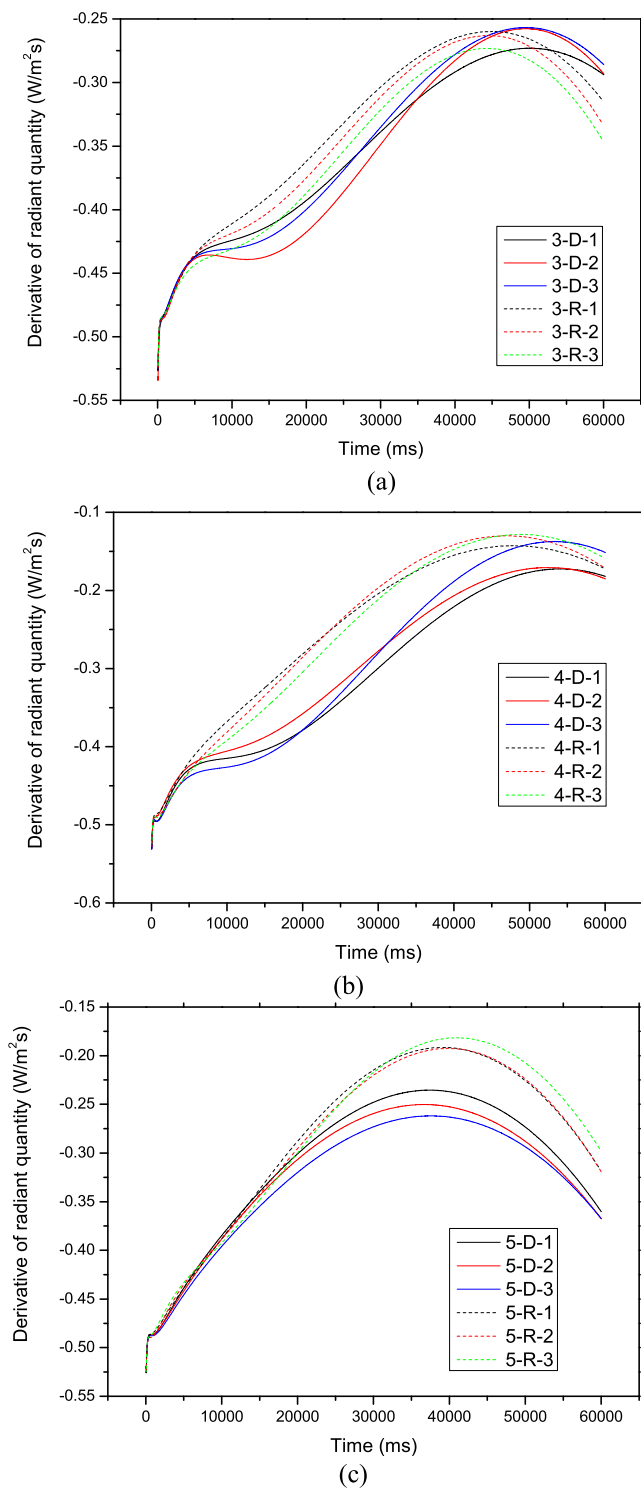
(a)

(b)

(c)

FIGURE 9. Radiation change rate of short insulators: (a) Radiation change rate of No.3 sample; (b) Radiation change rate of No.4 sample; (c) Radiation change rate of No.5. sample.

as reference, maximal deviation percentage of other points on samples is calculated. The calculation results are listed in Table 2:

As indicated, defect impacts the rate of radiation variation more evidently. According to the results in Table 2, 15% and
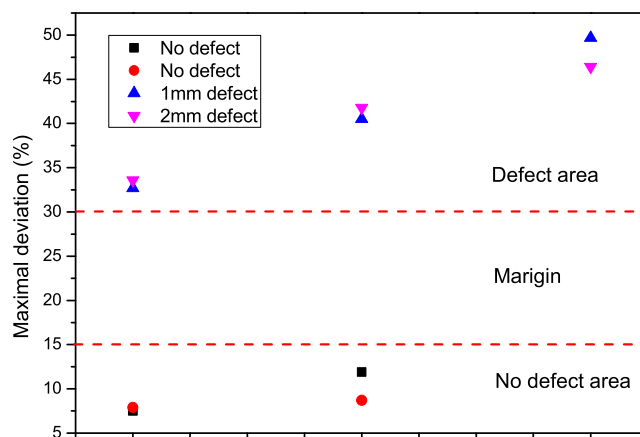

FIGURE 10. The test standard of the thermal wave methods.

TABLE 2. The maximal deviation percentage of test results.

No.	MD1[1] (%)	MD2[2] (%)	MD3[3] (%)	MD4[4] (%)
3	1.86-4.75	1.84-3.54	4.33-9.19	0.3-0.46
4	2.12-3.17	1.46-1.62	32.7-49.7	7.5-11.9
5	3.2-3.9	1.03-1.16	33.6-46.4	7.9-8.7

[1] MD1: Maximal deviation in defective area(radiation quantity) [2] MD2: Maximal deviation in reference area(radiation quantity) [3] MD3: Maximal deviation in defective area(rate of radiation quantity) [4] MD4: Maximal deviation in reference area(rate of radiation quantity)

30% could be chosen as standard for judgement respectively (see Fig.10). For deviation under 15%, no defect is deemed recognizable in inner insulator; when deviation is 15%-30%, inner defect dimension of insulator is less than 1mm; when deviation exceeds 30%, it can be deemed that there is evident air gap defect in composite insulators.

V. CONCLUSION

The manuscript has elucidated a type of NDT method based on the propagation law of heat to identify inner air gap in composite insulators. As proved by research results:

• After adding a transient thermal excitation to composite insulators, inner defect impacts heat transmission in samples so that radiation quantity of defect area outstrips that in non-defect area.

• Radiation variation is extremely rapid in early period and is comparatively slow in latter period. As no air gap impede heat transfer, the temperature in non-defect samples shall approach to balance temperature more rapidly. Therefore, the rate of radiation quantity of non-defect area is lower than that of defect area in latter period of test.

• Compared with radiation quantity, the rate of radiation quantity is more susceptible to defect. During the process of detection to insulator, taking minimum radiation quantity and absolute value of radiation variation rate as reference, maximal deviation quantity of other positions can be attained. For deviation under 15%, no defect is deemed recognizable

in insulator; when deviation is 15%-30%, inner defect dimension of insulator is less than 1mm; when deviation exceeds 30%, it can be deemed that there is evident that air gap defect is in insulator.

REFERENCES

[1] A. J. Phillips, A. J. Maxwell, C. S. Engelbrecht, and I. Gutman, "Electric-field limits for the design of grading rings for composite line insulators," *IEEE Trans. Power Del.*, vol. 30, no. 3, pp. 1110–1118, Jun. 2015, doi: 10.1109/TPWRD.2014.2362074.

[2] L. Yang *et al.*, "A recognition method of the hydrophobicity class of composite insulators based on features optimization and experimental verification," *Energies*, vol. 11, no. 4, p. 765, 2018, doi: 10.3390/en11040765.

[3] X. Zhang, J. Zhu, S. Bu, Q. Li, V. J. Terzija, and S. M. Rowlan, "The development of low-current surface arcs under clean and salt-fog conditions in electricity distribution networks," *IEEE Access*, vol. 6, pp. 15835–15843, 2018, doi: 10.1109/ACCESS.2018.2806885.

[4] B. Dong, X. Jiang, J. Hu, L. Shu, and C. Sun, "Effects of artificial polluting methods on AC flashover voltage of composite insulators," *IEEE Trans. Dielectr. Electr. Insul.*, vol. 19, no. 2, pp. 714–722, Apr. 2012, doi: 10.1109/TDEI.2012.6180267.

[5] B. Lutz, L. Cheng, Z. Guan, L. Wang, and F. Zhang, "Analysis of a fractured 500 kV composite insulator-identification of aging mechanisms and their causes," *IEEE Trans. Dielectr. Electr. Insul.*, vol. 19, no. 5, pp. 1723–1731, Oct. 2012, doi: 10.1109/TDEI.2012.6311521.

[6] Y. Tu *et al.*, "Moisture induced local heating of overhead line composite insulators," *IEEE Trans. Dielectr. Electr. Insul.*, vol. 24, no. 1, pp. 483–489, Feb. 2017, doi: 10.1109/TDEI.2016.005791.

[7] J. Wang, X. Liang, and Y. Gao, "Failure analysis of decay-like fracture of composite insulator," *IEEE Trans. Dielectr. Electr. Insul.*, vol. 21, no. 6, pp. 2503–2511, Dec. 2014, doi: 10.1109/TDEI.2014.004485.

[8] L. Cheng, L. Wang, Z. Guan, and F. Zhang, "Research on aged interfaces of composite insulators after extended water diffusion tests," *IEEE Trans. Dielectr. Electr. Insul.*, vol. 23, no. 6, pp. 3676–3682, Dec. 2016, doi: 10.1109/TDEI.2016.005793.

[9] K. Wieczorek and J. Fleszyński, "Steep-front impulse voltage in diagnostic studies of composite insulators," *IEEE Trans. Dielectr. Electr. Insul.*, vol. 23, no. 3, pp. 1236–1241, Jun. 2016, doi: 10.1109/TDEI.2015.005473.

[10] C. Yuan, C. Xie, L. Li, F. Zhang, and S. M. Gubanski, "Ultrasonic phased array detection of internal defects in composite insulators," *IEEE Trans. Dielectr. Electr. Insul.*, vol. 23, no. 1, pp. 525–531, Feb. 2016, doi: 10.1109/TDEI.2015.005225.

[11] J. Lee and Y. Cho, "Evaluation of interface defects in inaccessible reactor shrink fit nozzle welds using ultrasonic waves," *Energies*, vol. 10, no. 5, p. 589, 2017, doi: 10.3390/en10050589.

[12] C.-C. Cheng, T.-M. Cheng, and C.-H. Chiang, "Defect detection of concrete structures using both infrared thermography and elastic waves," *Autom. Construction*, vol. 18, pp. 87–92, Dec. 2008, doi: 10.1016/j.autcon.2008.05.004.

[13] N. Qaddoumi, A. H. El-Hag, M. A. Hosani, I. A. Mansouri, and H. A. Ghufli, "Detecting defects in outdoor non-ceramic insulators using near-field microwave non-destructive testing," *IEEE Trans. Dielectr. Electr. Insul.*, vol. 17, no. 2, pp. 402–407, Apr. 2010, doi: 10.1109/TDEI.2010.5448094.

[14] L. Cheng, R. Liao, L. Yang, and F. Zhang, "An optimized infrared detection strategy for defective composite insulators according to the law of heat flux propagation considering the environmental factors," *IEEE Access*, vol. 6, pp. 38137–38146, Jul. 2018, doi: 10.1109/ACCESS.2018.2854221.

[15] Y. Zhai, R. Chen, Q. Yang, X. Li, and Z. Zhao, "Insulator fault detection based on spatial morphological features of aerial images," *IEEE Access*, vol. 6, pp. 35316–35326, 2018, doi: 10.1109/ACCESS.2018.2846293.

[16] J. P. Holman, *Heat Transfer*, vol. 46. New York, NY, USA: McGraw-Hill, no. 3, 1985, pp. 121–130.

[17] X. Guo and Q. Fang, "Simulating thermal NDT of bonded structures by FEM," *Proc. SPIE*, vol. 6939, p. 69391H, Mar. 2008, doi: 10.1117/12.779942.

[18] L. Cheng, L. Wang, H. Mei, Z. Guan, and F. Zhang, "Research of nondestructive methods to test defects hidden within composite insulators based on THz time-domain spectroscopy technology," *IEEE Trans. Dielectr. Electr. Insul.*, vol. 23, no. 4, pp. 2126–2133, Aug. 2016, doi: 10.1109/TDEI.2016.7556487.

[19] P. D. Bastidas and S. M. Rowland, "Interfacial aging in composite insulators as a result of partial discharge activity," in *Proc. IEEE Electr. Insul. Conf.*, Baltimore, MD, USA, Jun. 2017, pp. 13–16.

[20] Z. Wang, L. H. Zhao, Z. D. Jia, and Z. C. Guan, "Performances of FRP core rod-HTV SIR sheath interface in a water environment," *IEEE Trans. Dielectr. Electr. Insul.*, vol. 24, no. 5, pp. 3024–3030, Oct. 2017, doi: 10.1109/TDEI.2017.006293.

[21] C. Xie, Z. He, Y. Lin, L. Li, and F. Zhang, "Using ultrasonic phased array to inspect the internal defects of composite insulators," *High Voltage Eng.*, vol. 40, no. 3, pp. 837–842, 2012.

[22] S. J. Wang, "Study on optimization design of shed configuration of AC composite insulators used in ice regions," Ph.D. dissertation, Dept. Elect. Eng., Chongqing Univ., Chongqing, China, 2015.

[23] F. L. Zhang, "Analysis on insulation performance discrepancy caused by vertical mold joint on surface of shed and sheath of silicone rubber composite insulator caused by injection mold," *Power Syst. Technol.*, vol. 24, no. 9, pp. 5–7, 2000.
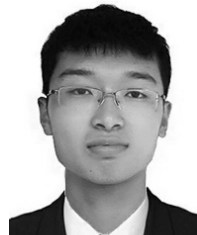
SIDA ZHANG was born in Dezhou, Shandong, China, in 1993. He received the B.S. degree in electrical engineering and automation from Chang'an University, Xi'an, China, in 2012. He is currently pursuing the Ph.D. degree in electrical engineering from Chongqing University, Chongqing, China. His research interests are nondestructive testing and HV outdoor insulation.

CHENJUN GUO was born in Kunming, Yunnan, China, in 1988. He received the B.S. and M.S. degrees in high voltage engineering from the Department of Electrical Engineering, Tsinghua University, Beijing, China, in 2011 and 2013, respectively. He is currently an Engineer at the Electric Power Research Institute, Yunnan Power Grid Co. Ltd. His research interests include high voltage test, transformer fault diagnosis, high voltage insulation, and evaluation of external insulation state.

LI CHENG was born in Chongqing, China, in 1989. He received the B.Sc. and Ph.D. degrees from the Department of Electrical Engineering, Tsinghua University, China, in 2011 and 2016, respectively. He is currently a Lecturer with Chongqing University. His research fields are nondestructive testing and HV outdoor insulation.
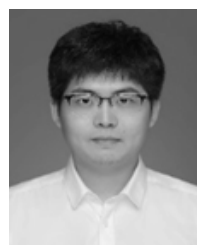
HANQING WANG was born in Jining, Shandong, China, in 1996. He received the B.S. degree in electrical engineering from Chongqing University, Chongqing, China, in 2018, where he is currently pursuing the Ph.D. degree in condition monitoring of power equipment.

• • •